2023 62nd IEEE Conference on Decision and Control (CDC)
December 13-15, 2023. Marina Bay Sands, Singapore

Distributed Observer-Based Dynamic Event-Triggered Control of Multi-Agent Systems with Adjustable Inter-Event Time

Zeyuan Wang and Mohammed Chadli

Abstract— **This paper proposes a dynamic event-triggered control strategy for the leader-following multi-agent control under directed topology. A synthesis approach combining distributed controllers and observers design is developed under a dynamic sampling scheme, and only local information is required for each agent to implement the proposed method. The control protocol incorporates model-based estimation and clock-like auxiliary dynamic variables to prolong the inter-event time as long as possible. Sufficient conditions for leader-following consensus control are established by linear matrix inequalities, and an explicit inter-event time is given to enable flexible tuning. Due to the carefully selected Lyapunov function, the proposed method exhibits significant advantages over the dynamic event-triggered control methods described in the existing literature. Compared to the existing static event-triggered strategy, the proposed approach significantly reduces the utilization of communication resources while preserving asymptotic convergence to the state consensus. The validity and effectiveness of the proposed theoretical results are demonstrated by comparative simulations.**

I. INTRODUCTION

Advancements in technology have highlighted the significance of cooperative control issues in multi-agent systems (MASs). As the core of cooperative control, consensus issues have been widely studied and applied in engineering practice in recent years. One of the particularly intriguing topics is leader-following control, where a group of agents needs to achieve consensus with a leader agent. This topic has been extensively explored for both linear [1] and nonlinear MASs [2], and for MASs comprising homogeneous or heterogeneous agents [3]. The techniques used for leader-following consensus can also be extended to formation control such as in [4].

In time-triggered control systems, control updates and data transmissions occur periodically. This can lead to an excessive burden on communication networks and an increase in computing resources for MASs [5]. In order to address this issue, an event-triggered mechanism (ETM) was introduced, which enables a minimum rate of data sampling, communication, and control updates while still ensuring system performance. The concept of ETM for stabilizing control is first introduced in [6], then gains significant development and is applied in different dynamic systems [7], [8].

This work was supported by the China Scholarship Council under Grant 202206020096.

Zeyuan Wang is with University Paris-Saclay, Univ Evry, IBISC, 91020 Evry, France zeyuan.wang@universite-paris-saclay.fr

Mohammed Chadli is with University Paris-Saclay, Univ Evry, IBISC, 91020 Evry, France mohammed.chadli@univ-evry.fr

In order to increase the inter-event time (IET), a dynamic event-triggered mechanism (DETM) was proposed in [9], where the event's threshold value is dynamically changing, which makes it different from the former static one. The DETM has been successfully applied in MASs in many different scenarios [10], [11], [12]. In the literature [10] and [13], auxiliary dynamic variables (ADVs) are introduced as clock-like variables, providing more freedom to select a preferred (minimum) IET by choosing appropriate parameters in the controller design phase; thus, the Zeno behavior of MAS is excluded, though the rigorous proof of the minimum IET (MIET) is still challenging without enforcing a dwell-time [13]. This method is extended in [14] with an improved DETM based on a moving average approach. A more generic result is proposed for nonlinear systems in [15].

The physical state of most real systems cannot be determined by direct measurement. Therefore, state observers become necessary to estimate the system's internal states based on its inputs and outputs. Observers for MASs entail a co-design problem that involves event-triggered control and estimation. There have been some studies that address this issue. In the literature [16], the control/observer co-design problem for generic linear MASs for leaderless consensus is studied. The results are then developed in [17] for the leader-following problem but only apply to second-order linear MASs. In the literature [18], an observer-based ETM is proposed to deal with formation control problems under switching and directed topology. A more generic approach is proposed in [19], which uses linear matrix inequalities ($\mathcal{LMI}$s) to synthesize the controller and observer, but the solution is not distributed. The aforementioned studies are based on static event-triggered control, with few utilizing DETMs. Notably, the literature in [20] and [11] designs observers-based DETM control while also eliminating the Zeno behavior. However, the complexity of parameter tuning presents a challenge in designing the MIET quantitatively. Based on the above discussion, the synthesis of a distributed controller and observer under DETM with adjustable MIET has yet to be fully explored.

This work is inspired by [13], [10], [15], where DETMs are realized based on clock-like ADVs to facilitate the MIET adjustment. However, in [10], a discontinuous Lyapunov function chosen will fail to achieve leader-following consensus. The resulting DETM only guarantees stability between two consecutive events, though the authors did not report this remark. Based on the above discussion, we improve the DETM in [10] by introducing a new continuous Lyapunov function and propose a novel distributed controller/observer synthesis method using the $\mathcal{LMI}$ approach, which is developed under a directed communication topology. This method significantly reduces the frequency of information exchange and communication updates while ensuring asymptotic convergence of the system. The mechanism allows the adjustment of the minimum inter-event time by tuning the upper bound of the auxiliary dynamic variables and guarantees a Zeno-free operation.

The rest of the paper is structured as follows: In section II, we provide notations and the problem formulation. Section III presents the design of distributed dynamic event-triggered control, including the controller/observer synthesis and rigorous proof of adjustable MIET. We demonstrate the effectiveness of the proposed strategies through numerical simulations and discuss the results in section IV. The main conclusion is presented in section V.

II. PRELIMINARIES AND PROBLEM STATEMENT

A. Preliminaries

Let $\mathbb{R}$ denote the set of real numbers. Let $\mathbb{N}^+$ denote the set of positive natural numbers. Given a matrix $\boldsymbol{E}$, $\boldsymbol{E}^T$ denotes its transpose. If $\boldsymbol{E}$ is a square matrix, $\lambda_{\min}(\boldsymbol{E})$ and $\lambda_{\max}(\boldsymbol{E})$ denote the minimum and maximum eigenvalues of $\boldsymbol{E}$ respectively, and $\boldsymbol{E}^{-1}$ (resp. $\boldsymbol{E}^{-T}$) represents its inverse (resp. the transpose of the inverse). For a symmetric matrix $\boldsymbol{E}$, $\boldsymbol{E} < 0 (\leq 0)$ denotes that $\boldsymbol{E}$ is negative definite (negative semi-definite), and $\boldsymbol{E} > 0 (\geq 0)$ means $-\boldsymbol{E} < 0 (\leq 0)$. $\boldsymbol{I}_n$ denotes an identity matrix of dimension n. $\mathbf{0}_{m\times n}$ (resp. $\mathbf{0}_n$) denotes a zero matrix of dimension $m\times n$ (resp. of dimension $n\times n$). $\otimes$ denotes the Kronecker product. $\|\cdot\|$ denotes ℓ_2-norm for vectors or spectrum norm for matrices. Let $*$ denote the symmetric entries in a matrix.

The communication topology of N ($N \in \mathbb{N}^+$) follower agents is represented by a directed graph $\mathcal{G} = (\mathcal{V}, \mathcal{E})$ consisting of a vertex set $\mathcal{V} = \{v_1, ..., v_N\}$ and an edge set $\mathcal{E} \subseteq \mathcal{V} \times \mathcal{V}$. Follower agent i and the leader are represented as vertices v_i and v_0, respectively. Denote $\mathcal{N}_i$ the set of neighbors of agent i. The weighted adjacency matrix $\boldsymbol{\mathcal{A}} = (a_{ij}) \in \mathbb{R}^{N\times N}$ of $\mathcal{G}$ is defined such that $a_{ii} = 0$, $a_{ij} = 1$ if v_i is connected to v_j (i.e., there exists a directed edge (v_i, v_j) from v_j to v_i) and $a_{ij} = 0$ otherwise. The Laplacian matrix $\boldsymbol{\mathcal{L}} = (l_{ij}) \in \mathbb{R}^{N\times N}$ is defined as $l_{ii} = \sum_{i\neq j} a_{ij}$ and $l_{ij} = -a_{ij}, i \neq j$. Define $\bar{\mathcal{G}} = (\bar{\mathcal{V}}, \bar{\mathcal{E}})$ the augmented graph of $\mathcal{G}$, with $\bar{\mathcal{V}} = \mathcal{V} \cup \{v_0\}$ and $(v_i, v_0) \in \bar{\mathcal{E}}$ if agent i is connected to the leader. Define leader adjacency matrix $\boldsymbol{\mathcal{D}} = \mathrm{diag}(d_1, ..., d_N)$ as a diagonal matrix where its diagonal element $d_i = 1$ if $(v_i, v_0) \in \bar{\mathcal{E}}$ otherwise $d_i = 0$. Define $\boldsymbol{\mathcal{H}} = \boldsymbol{\mathcal{L}} + \boldsymbol{\mathcal{D}}$.

B. Problem Statement

Consider a linear MAS with N ($N \in \mathbb{N}^+$) follower agents and one leader represented by

$$\begin{cases} \dot{\boldsymbol{x}}_i(t) = \boldsymbol{A}\boldsymbol{x}_i(t) + \boldsymbol{B}\boldsymbol{u}_i(t), \quad i = 1, ..., N \\ \boldsymbol{y}_i(t) = \boldsymbol{C}\boldsymbol{x}_i(t), \quad i = 1, ..., N \\ \dot{\boldsymbol{x}}_0(t) = \boldsymbol{A}\boldsymbol{x}_0(t) \end{cases} \tag{1}$$

where $\boldsymbol{x}_i(t), i = 1, ..., N$ and $\boldsymbol{x}_0(t)$ denote the states of follower agents and the leader, respectively. $\boldsymbol{y}_i(t)$ is the output of agent i, $\boldsymbol{u}_i(t) \in \mathbb{R}^m$ is the control input of agent i. $\boldsymbol{A} \in \mathbb{R}^{n\times n}, \boldsymbol{B} \in \mathbb{R}^{n\times m}$, $\boldsymbol{C} \in \mathbb{R}^{r\times n}$. Define the consensus error of agent i as $\boldsymbol{\xi}_i(t) = \boldsymbol{x}_i(t) - \boldsymbol{x}_0(t)$ and $\boldsymbol{\xi}(t) = [\boldsymbol{\xi}_1^T(t), ..., \boldsymbol{\xi}_N^T(t)]^T$. The objective of this study is to design an event-based control law such that all follower agents and the leader achieve the state consensus, i.e.,

$$\lim_{t\to\infty} \|\boldsymbol{\xi}_i(t)\| = 0, \forall i \in \{1, ..., N\} \tag{2}$$

In order to estimate the agents' internal states, Luenberger-type observers are designed for each follower agent i to reconstruct the state $\boldsymbol{x}_i(t)$ from the output $\boldsymbol{y}_i(t)$ and the input $\boldsymbol{u}_i(t)$:

$$\begin{cases} \dot{\tilde{\boldsymbol{x}}}_i(t) = \boldsymbol{A}\tilde{\boldsymbol{x}}_i(t) + \boldsymbol{B}\boldsymbol{u}_i(t) + \boldsymbol{L}_o(\tilde{\boldsymbol{y}}_i(t) - \boldsymbol{y}_i(t)) \\ \tilde{\boldsymbol{y}}_i(t) = \boldsymbol{C}\tilde{\boldsymbol{x}}_i(t) \end{cases} \tag{3}$$

where $\boldsymbol{L}_o \in \mathbb{R}^{n\times r}$ is the gain to be designed, and $\tilde{\boldsymbol{x}}_i(t)$ is the observer state. Define observer error of agent i as $\boldsymbol{\zeta}_i(t) = \tilde{\boldsymbol{x}}_i(t) - \boldsymbol{x}_i(t)$ and $\boldsymbol{\zeta}(t) = [\boldsymbol{\zeta}_1^T(t), ..., \boldsymbol{\zeta}_N^T(t)]^T$.

The following assumptions hold in this paper:

Assumption 1: The leader's states are accessible.

In practical engineering, leaders are usually specially designed or virtual, and we can directly access the state of the leader.

Assumption 2: $(\boldsymbol{A}, \boldsymbol{B}, \boldsymbol{C})$ is stabilizable and observable.

Assumption 3: The graph $\mathcal{G}$ is fixed and directed. Furthermore, the augmented graph $\bar{\mathcal{G}}$ contains a spanning tree with the leader agent being its root.

Under Assumption 3, we recall the following property of matrix $\boldsymbol{\mathcal{H}}$ due to [21]:

Lemma 1: There exists a positive diagonal matrix $\boldsymbol{\Psi} = \mathrm{diag}(\psi_1, ..., \psi_N) > 0$ such that $\boldsymbol{\Psi}\boldsymbol{\mathcal{H}} + \boldsymbol{\mathcal{H}}^T\boldsymbol{\Psi} > 0$.

The proposed event-triggered control input $\boldsymbol{u}_i(t)$ of agent i is defined as

$$\begin{cases} \boldsymbol{u}_i(t) = \boldsymbol{K}\boldsymbol{z}_i(t) \\ \boldsymbol{z}_i(t) = \sum\limits_{j\in\mathcal{N}_i} a_{ij}(\hat{\boldsymbol{x}}_j(t) - \hat{\boldsymbol{x}}_i(t)) + d_i(\boldsymbol{x}_0(t) - \hat{\boldsymbol{x}}_i(t)) \end{cases} \tag{4}$$

where $\boldsymbol{K} \in \mathbb{R}^{m\times n}$ is the gain of the feedback control, $\boldsymbol{z}_i(t)$ is the combinatory state. Define $\boldsymbol{z}(t) = [\boldsymbol{z}_1^T(t), ..., \boldsymbol{z}_N^T(t)]^T$. $\hat{\boldsymbol{x}}_i(t), i \in \{1, ..., N\}$ is defined as:

$$\hat{\boldsymbol{x}}_i(t_k^i) = \tilde{\boldsymbol{x}}_i(t_k^i) \text{ and } \frac{d}{dt}\hat{\boldsymbol{x}}_i(t) = \boldsymbol{A}\hat{\boldsymbol{x}}_i(t),\ t \in [t_k^i, t_{k+1}^i) \tag{5}$$

where $\tilde{\boldsymbol{x}}_i(t_k^i)$ is the observer state at the last triggering moment t_k^i, and t_{k+1}^i is defined by event-triggered rules given in the following section. Define measurement error of agent i as $\boldsymbol{e}_i(t) = \hat{\boldsymbol{x}}_i(t) - \tilde{\boldsymbol{x}}_i(t)$ and $\boldsymbol{e}(t) = [\boldsymbol{e}_1^T(t), ..., \boldsymbol{e}_N^T(t)]^T$.

Remark 1: The term $\hat{\boldsymbol{x}}_i(t) = \tilde{\boldsymbol{x}}_i(t_k^i)e^{\boldsymbol{A}(t-t_k^i)}$ is a kind of model-based estimation [22]. Since the trivial estimation $\hat{\boldsymbol{x}}_i(t) = \tilde{\boldsymbol{x}}_i(t_k^i)$ may differ from $\tilde{\boldsymbol{x}}_i(t)$ very quickly, the exponential term $e^{\boldsymbol{A}}$ with agent's dynamic matrix $\boldsymbol{A}$ is used to reduce the error between $\hat{\boldsymbol{x}}_i(t)$ and $\tilde{\boldsymbol{x}}_i(t)$ thus usually increases the inter-event time.

By definition of $\boldsymbol{\xi}_i(t)$, $\boldsymbol{\zeta}_i(t)$ and $\boldsymbol{e}_i(t)$, we can deduce $\boldsymbol{z}_i(t)$ as

$$\boldsymbol{z}_i = \sum_{j\in\mathcal{N}_i} a_{ij}(\boldsymbol{e}_j - \boldsymbol{e}_i + \boldsymbol{\zeta}_j - \boldsymbol{\zeta}_i + \boldsymbol{\xi}_j - \boldsymbol{\xi}_i) + d_i(-\boldsymbol{e}_i - \boldsymbol{\zeta}_i - \boldsymbol{\xi}_i) \tag{6}$$

then we can have $\boldsymbol{z} = -(\boldsymbol{\mathcal{H}} \otimes \boldsymbol{I}_n)(\boldsymbol{e} + \boldsymbol{\zeta} + \boldsymbol{\xi})$ and the following expressions:

$$\begin{cases} \dot{\boldsymbol{\xi}} = (\boldsymbol{I}_N \otimes \boldsymbol{A} - \boldsymbol{\mathcal{H}} \otimes \boldsymbol{BK})\boldsymbol{\xi} - (\boldsymbol{\mathcal{H}} \otimes \boldsymbol{BK})(\boldsymbol{\zeta} + \boldsymbol{e}) \\ \dot{\boldsymbol{\zeta}} = (\boldsymbol{I}_N \otimes (\boldsymbol{A} + \boldsymbol{L}_o\boldsymbol{C}))\boldsymbol{\zeta} \\ \dot{\boldsymbol{e}} = (\boldsymbol{\mathcal{H}} \otimes \boldsymbol{BK})\boldsymbol{\xi} + (\boldsymbol{I}_N \otimes \boldsymbol{A} + \boldsymbol{\mathcal{H}} \otimes \boldsymbol{BK})\boldsymbol{e} \\ \qquad + (\boldsymbol{\mathcal{H}} \otimes \boldsymbol{BK} - \boldsymbol{I}_N \otimes \boldsymbol{L}_o\boldsymbol{C})\boldsymbol{\zeta} \end{cases} \tag{7}$$

III. MAIN RESULTS

A. Observer and controller synthesis for distributed dynamic event-triggered control

This section proposes a distributed design of controllers and observers for follower agents and the DETM rule to determine the non-periodic data transmission protocol.

Theorem 1: The MAS described in (1) achieves leader-following consensus under the control law defined in (4) if there exist scalars $b_1 > 0$ and $b_2 > 0$, matrices $\boldsymbol{P}_1 > 0$, $\boldsymbol{P}_2 > 0$, the controller gain $\boldsymbol{K}$ and the observer gain $\boldsymbol{L}_o$ satisfying the following inequality matrix:

$$\boldsymbol{S} = \begin{pmatrix} \boldsymbol{S}_{11} & \boldsymbol{S}_{12} \\ * & \boldsymbol{S}_{22} \end{pmatrix} < 0 \tag{8}$$

where $\boldsymbol{S}_{11}$, $\boldsymbol{S}_{12}$ and $\boldsymbol{S}_{22}$ are defined as

$$\begin{cases} \boldsymbol{S}_{11} = \boldsymbol{\Psi} \otimes (\boldsymbol{P}_1\boldsymbol{A} + \boldsymbol{A}^T\boldsymbol{P}_1) - (\boldsymbol{\Psi}\boldsymbol{\mathcal{H}}) \otimes \boldsymbol{P}_1\boldsymbol{BK} \\ \qquad - (\boldsymbol{\mathcal{H}}^T\boldsymbol{\Psi}) \otimes \boldsymbol{K}^T\boldsymbol{B}^T\boldsymbol{P}_1 \\ \boldsymbol{S}_{12} = -(\boldsymbol{\Psi}\boldsymbol{\mathcal{H}}) \otimes (\boldsymbol{P}_1\boldsymbol{BK}) \\ \boldsymbol{S}_{22} = \boldsymbol{\Psi} \otimes (\boldsymbol{P}_2\boldsymbol{A} + \boldsymbol{A}^T\boldsymbol{P}_2 + \boldsymbol{P}_2\boldsymbol{L}_o\boldsymbol{C} + \boldsymbol{C}^T\boldsymbol{L}_o^T\boldsymbol{P}_2) \\ \qquad + (b_1 + b_2)\boldsymbol{I}_{Nn} \end{cases} \tag{9}$$

and the matrix $\boldsymbol{\mathcal{H}}$ given by the associated topology, and the matrix $\boldsymbol{\Psi}$ satisfying Lemma 1.

The event-triggered rule of agent i is defined as

$$\begin{aligned} & t_{k+1}^i \triangleq \inf\left\{t > t_k^i \mid \theta_i(t) \le 0\right\}, \ \theta_i(t_k^i) = \bar{\theta}_i \\ & \dot{\theta}_i(t) = \begin{cases} \min(\omega_i(t), 0) - \tau_i & \text{if } \|\boldsymbol{e}_i(t)\| \neq 0 \\ -\tau_i & \text{otherwise} \end{cases} \end{aligned} \tag{10}$$

where $\bar{\theta}_i > 0$, $\tau_i > 0$, and $\omega_i(t)$ is defined as:

$$\begin{aligned} \omega_i(t) \triangleq & -\frac{1}{\Pi_{3i}}\left[\boldsymbol{e}_i^T\boldsymbol{Q}\boldsymbol{e}_i + \epsilon\left(\frac{1}{k} - \frac{\bar{\delta}_{\min}}{2}\right)\|\boldsymbol{z}_i\|^2 \right. \\ & \left. + \boldsymbol{e}_i^T(2\psi_i\boldsymbol{M}_1 - 2\psi_i\theta_i\boldsymbol{M}_3)\boldsymbol{z}_i\right] \end{aligned} \tag{11}$$

with $\Pi_{3i} = \boldsymbol{\psi}_i e_i^T\boldsymbol{P}_3\boldsymbol{e}_i$, and

$$\begin{aligned} \boldsymbol{Q} = & \left(\epsilon k\|\boldsymbol{\mathcal{H}}^{-1}\|^2 - \frac{\epsilon}{2} + 2\psi_{\max}\|\boldsymbol{\mathcal{H}}\|^2\|\boldsymbol{M}_1\|\right)\boldsymbol{I}_n \\ & + 2\psi_i\theta_i\boldsymbol{P}_3\boldsymbol{A} \\ & + \frac{\psi_{\max}\|\boldsymbol{\mathcal{H}}\|^2}{b_1}\boldsymbol{M}_1^T\boldsymbol{M}_1 + \frac{\psi_i^2\theta_i^2}{b_2}\boldsymbol{M}_2^T\boldsymbol{M}_2 \end{aligned} \tag{12}$$

and $\boldsymbol{M}_1 = \boldsymbol{K}^T\boldsymbol{B}^T\boldsymbol{P}_1$, $\boldsymbol{M}_2 = \boldsymbol{P}_3\boldsymbol{L}_o\boldsymbol{C}$, $\boldsymbol{M}_3 = \boldsymbol{P}_3\boldsymbol{BK}$, $\psi_{\max} = \|\boldsymbol{\Psi}\|$, $\bar{\delta}_{\min} = \lambda_{\min}(\boldsymbol{\mathcal{H}}^{-T}\boldsymbol{\mathcal{H}}^{-1})$, $k > 2/\bar{\delta}_{\min}$, $\boldsymbol{P}_3 > 0$. $\epsilon > 0$ is a scalar satisfying $\boldsymbol{S} + \epsilon\boldsymbol{I} \le 0$.

Proof: Due to page limits, we can only provide a brief proof and key ideas of this theorem. It consists of showing the stability of the closed-loop system (7) by using Lyapunov theorem. We choose the following Lyapunov function $V(t)$: $V(t) = V_1(t) + V_2(t) + V_3(t)$ where $V_1(t) = \boldsymbol{\xi}(t)^T(\boldsymbol{\Psi} \otimes \boldsymbol{P}_1)\boldsymbol{\xi}(t)$, $V_2(t) = \boldsymbol{\zeta}(t)^T(\boldsymbol{\Psi} \otimes \boldsymbol{P}_2)\boldsymbol{\zeta}(t)$ and $V_3(t) = \boldsymbol{e}(t)^T(\boldsymbol{\Psi}\boldsymbol{\Theta}(t) \otimes \boldsymbol{P}_3)\boldsymbol{e}(t)$, with $\boldsymbol{P}_1, \boldsymbol{P}_2, \boldsymbol{P}_3$ are all positive definite, $\boldsymbol{\Psi} = \text{diag}(\psi_1, ..., \psi_N)$ satisfying Lemma 1, $\boldsymbol{\Theta}(t) = \text{diag}(\theta_1(t), ..., \theta_N(t)) > 0$, and $\dot{\boldsymbol{\Theta}}(t) < 0$ by definition of event-triggered rule (10), thus $V(t) \ge 0$. The rest of the proof is to study the derivative of $V(t)$, and apply Cauchy–Schwarz inequalities and matrix diagonalization to obtain a decoupled summation of functions of each agent, leading to a final expression of $\dot{V}(t)$: $\dot{V}(t) \le \sum_{i=1}^N \left(\boldsymbol{e}_i^T\boldsymbol{Q}\boldsymbol{e}_i + \Pi_1\|\boldsymbol{z}_i\|^2 + \boldsymbol{e}_i^T\boldsymbol{\Pi}_{2i}\boldsymbol{z}_i + \Pi_{3i}\dot{\theta}_i\right)$, where $\boldsymbol{Q}$ is defined in (12), $\Pi_1 = \epsilon(\frac{1}{k} - \frac{1}{2}\bar{\delta}_{\min})$, $\boldsymbol{\Pi}_{2i} = -2\psi_i\theta_i\boldsymbol{M}_3 + 2\psi_i\boldsymbol{M}_1$ and $\Pi_{3i} = \boldsymbol{\psi}_i\boldsymbol{e}_i^T\boldsymbol{P}_3\boldsymbol{e}_i$. By substituting $\dot{\theta}_i$ in (10) in $\dot{V}(t)$ and we get $\dot{V}(t) \le -\sum_i \tau_i < 0$. Therefore, the closed-loop system (7) is asymptotically stable and the MAS achieves consensus. ■

The difficulty of Theorem 1 lies in determining $\boldsymbol{K}$ and $\boldsymbol{L}_o$, which involves a set of bilinear matrix inequalities ($\mathcal{BMIs}$) (8). These equations can be challenging to solve and may need a lot of attempts through numerical iterations. In the following corollary, sufficient conditions of $\mathcal{LMIs}$ to solve $\mathcal{BMIs}$ in Theorem 1 are proposed, which simplifies numerical computation.

Corollary 1: The design conditions of Theorem 1 are satisfied if there exist $\boldsymbol{P}_1 > 0$, $\boldsymbol{P}_2 > 0$, $\boldsymbol{K}$ and $\boldsymbol{F}$ satisfying the following $\mathcal{LMIs}$ conditions:

$$\boldsymbol{\Omega} = \begin{pmatrix} \boldsymbol{\Omega}_{11} & \boldsymbol{0}_{Nn} & \boldsymbol{\Omega}_{13} & \boldsymbol{\Omega}_{14} \\ * & \boldsymbol{\Omega}_{22} & -\boldsymbol{I}_N \otimes \boldsymbol{K}^T & \boldsymbol{0}_{Nn} \\ * & * & -2\boldsymbol{I}_{Nm} & \boldsymbol{0}_{Nm\times Nn} \\ * & * & * & -\boldsymbol{I}_{Nn} \end{pmatrix} < 0 \tag{13}$$

where $\boldsymbol{\Omega}_{11}$, $\boldsymbol{\Omega}_{13}$, $\boldsymbol{\Omega}_{14}$, $\boldsymbol{\Omega}_{22}$ are defined as

$$\begin{cases} \boldsymbol{\Omega}_{11} = \boldsymbol{\Psi} \otimes (\boldsymbol{P}_1\boldsymbol{A} + \boldsymbol{A}^T\boldsymbol{P}_1) + \boldsymbol{I}_{Nn} - 2\dfrac{\boldsymbol{I}_N \otimes \boldsymbol{P}_1}{\mu_1} \\ \boldsymbol{\Omega}_{13} = (\boldsymbol{\Psi}\boldsymbol{\mathcal{H}}) \otimes (\boldsymbol{P}_1\boldsymbol{B}) \\ \boldsymbol{\Omega}_{14} = \dfrac{\boldsymbol{I}_N \otimes \boldsymbol{P}_1}{\mu_1} - \mu_1(\boldsymbol{\Psi}\boldsymbol{\mathcal{H}}) \otimes (\boldsymbol{K}^T\boldsymbol{B}^T) \\ \boldsymbol{\Omega}_{22} = \boldsymbol{\Psi} \otimes (\boldsymbol{P}_2\boldsymbol{A} + \boldsymbol{A}^T\boldsymbol{P}_2 + \boldsymbol{FC} + \boldsymbol{C}^T\boldsymbol{F}^T) \\ \qquad + (b_1 + b_2)\boldsymbol{I}_{Nn} \end{cases} \tag{14}$$

where $b_1 > 0$, $b_2 > 0$, and $\mu_1 > 0$ are arbitrary positive scalars. Then the observer gain is obtained as $\boldsymbol{L}_o = \boldsymbol{P}_2^{-1}\boldsymbol{F}$.

Proof: We first make a change of variable of $\boldsymbol{F} = \boldsymbol{P}_2\boldsymbol{L}_o$ thus the term $\boldsymbol{S}_{22}$ in $\boldsymbol{S}$ (8) becomes $\boldsymbol{\Omega}_{22}$. Notice that the matrix $\boldsymbol{S}$ in (1) could be decomposed into $\boldsymbol{S} = \boldsymbol{\Gamma}^T\boldsymbol{\Lambda}\boldsymbol{\Gamma}$

with $\boldsymbol{\Gamma}$ and $\boldsymbol{\Lambda}$ defined as

$$\boldsymbol{\Gamma} = \begin{pmatrix} \boldsymbol{I}_{Nn} & \boldsymbol{0}_{Nn} \\ \boldsymbol{0}_{Nn} & \boldsymbol{I}_{Nn} \\ \boldsymbol{0}_{Nm\times Nn} & -\boldsymbol{I}_N \otimes \boldsymbol{K} \end{pmatrix} \tag{15}$$

$$\boldsymbol{\Lambda} = \begin{pmatrix} \boldsymbol{\Lambda}_{11} & \boldsymbol{0}_{Nn} & \boldsymbol{\mathcal{H}} \otimes \boldsymbol{P}_1\boldsymbol{B} \\ * & \boldsymbol{\Omega}_{22} & -\boldsymbol{I}_N \otimes \boldsymbol{K}^T \\ * & * & -2\boldsymbol{I}_{Nn} \end{pmatrix} \tag{16}$$

where $\boldsymbol{\Lambda}_{11} = \boldsymbol{I}_N \otimes (\boldsymbol{P}_1\boldsymbol{A} + \boldsymbol{A}^T\boldsymbol{P}_1) - \boldsymbol{\mathcal{H}} \otimes (\boldsymbol{P}_1\boldsymbol{B}\boldsymbol{K} + \boldsymbol{K}^T\boldsymbol{B}^T\boldsymbol{P}_1)$. Then, $\boldsymbol{\Lambda} < 0$ becomes a sufficient condition for $\boldsymbol{S} < 0$. To find a $\mathcal{LMI}$ form, the idea is to separate $\boldsymbol{P}_1$ and $\boldsymbol{K}$ in $\boldsymbol{\Lambda}_{11}$. We use the following inequalities: $-\boldsymbol{\mathcal{H}} \otimes (\boldsymbol{P}_1\boldsymbol{B}\boldsymbol{K} + \boldsymbol{K}^T\boldsymbol{B}^T\boldsymbol{P}_1) \leq -\boldsymbol{\mathcal{H}} \otimes (\boldsymbol{P}_1\boldsymbol{B}\boldsymbol{K} + \boldsymbol{K}^T\boldsymbol{B}^T\boldsymbol{P}_1) + \mu_1^2\boldsymbol{\mathcal{H}}^2 \otimes \boldsymbol{K}^T\boldsymbol{B}^T\boldsymbol{B}\boldsymbol{K} \leq (\boldsymbol{I}_N \otimes \boldsymbol{P}_1/\mu_1 - \mu_1\boldsymbol{\mathcal{H}} \otimes \boldsymbol{B}\boldsymbol{K})^T(\boldsymbol{I}_N \otimes \boldsymbol{P}_1/\mu_1 - \mu_1\boldsymbol{\mathcal{H}} \otimes \boldsymbol{B}\boldsymbol{K}) - \boldsymbol{I}_N \otimes \boldsymbol{P}_1^2/\mu_1^2, \mu_1 > 0$. Notice that $-\boldsymbol{I}_N \otimes \boldsymbol{P}_1^2/\mu_1^2 \leq \boldsymbol{I}_{Nn} - 2(\boldsymbol{I} \otimes \boldsymbol{P}_1)/\mu_1$, then we have $-\boldsymbol{\mathcal{H}} \otimes (\boldsymbol{P}_1\boldsymbol{B}\boldsymbol{K} + \boldsymbol{K}^T\boldsymbol{B}^T\boldsymbol{P}_1) \leq (\boldsymbol{I}_N \otimes \boldsymbol{P}_1/\mu_1 - \mu_1\boldsymbol{\mathcal{H}} \otimes \boldsymbol{B}\boldsymbol{K})^T(\boldsymbol{I}_N \otimes \boldsymbol{P}_1/\mu_1 - \mu_1\boldsymbol{\mathcal{H}} \otimes \boldsymbol{B}\boldsymbol{K}) + \boldsymbol{I}_{Nn} - 2(\boldsymbol{I} \otimes \boldsymbol{P}_1)/\mu_1$ Thus by replacing this inequality for $\boldsymbol{\Lambda}_{11}$ in $\boldsymbol{\Lambda}$ (16) and the Schur complement, we can obtain the matrix $\boldsymbol{\Omega}$ in (13). ■

Remark 2: The Lyapunov function proposed in the proof of Theorem 1 is a continuous function, and the disadvantage of handling the discontinuity in the study [10] is naturally avoided. Notice that V_1 and V_2 are continuous since $\boldsymbol{\xi}$ and $\boldsymbol{\zeta}$ are continuous. In V_3, although $\boldsymbol{e}(t)$ and $\boldsymbol{\Psi}(t)$ are discontinuous at triggering moments, we can calculate the left-hand limit and right-hand limit of V_3, and since the left-hand limit of $\boldsymbol{\Psi}(t)$ (the corresponding component of triggered agent) and the right-hand limit of $\boldsymbol{e}(t)$ (of triggered agent) are both 0, V_3 is continuous and thus V is continuous.

Remark 3: Notice that this strategy is distributed; thus, each agent determines its triggering moments according to its local information, which also facilitates algorithm implementation.

B. Quantization of minimum inter-event time

The following corollary deduces an explicit MIET and proves that the Zeno behavior does not exist under Theorem (1).

Corollary 2: Under Theorem 1, the inter-event time of agent i is lower-bounded by $t^i_{\min}$ defined as

$$t^i_{\min} = \int_0^{h=\bar{\theta}_i} \frac{dh}{\max(c_0 + c_1 h + c_2 h^2, 0) + \tau_i} \tag{17}$$

where

$$\begin{cases} c_0 = \left(\epsilon k\|\boldsymbol{\mathcal{H}}^{-1}\|^2 - \dfrac{\epsilon}{2} + \dfrac{\psi_{\max}\|\boldsymbol{\mathcal{H}}\|^2\|\boldsymbol{M}_1\|^2}{b_1} \right. \\ \qquad \left. +2\psi_{\max}\|\boldsymbol{\mathcal{H}}\|\|\boldsymbol{M}_1\| + \dfrac{\psi_i\|\boldsymbol{M}_1\|^2}{\sigma_1}\right)\dfrac{1}{\psi_i\eta} \\ c_1 = \dfrac{\alpha}{\eta} \\ c_2 = \dfrac{1}{\eta}(\dfrac{\psi_i\|\boldsymbol{M}_2\|^2}{b_2} + \dfrac{\|\boldsymbol{M}_3\|^2}{\sigma_2}) \\ \alpha = \lambda_{\max}(\boldsymbol{P}_3\boldsymbol{A} + \boldsymbol{A}^T\boldsymbol{P}_3), \quad \eta = \lambda_{\min}(\boldsymbol{P}_3) \end{cases} \tag{18}$$

with $\boldsymbol{M}_1, \boldsymbol{M}_2, \boldsymbol{M}_3$ defined in Theorem 1, $k > 2/\bar{\delta}_{\min}$, and σ_1, σ_2 are two positive scalars satisfying $\frac{\epsilon\bar{\delta}_{\min}}{2} - \frac{\epsilon}{k} - \psi_i(\sigma_1 + \sigma_2) = 0$.

Proof: Due to page limit we can only provide a brief proof. Notice that the IET is determined by the evolution of $\theta_i(t)$ and is equal to the time required of $\theta_i(t)$ decreasing from $\bar{\theta}_i$ to 0. By analyzing the lower bound of $\boldsymbol{Q}$ and Π_{3i} in (11), we can obtain $\omega_i \geq -(c_0 + c_1\theta_i + c_2\theta_i^2)$. Then by definition of $\dot{\theta}_i(t)$ in (10), we can conclude that the time required for θ_i descending from $\bar{\theta}_i$ to 0 is lower bounded by $t^i_{\min} = \int_{h=\bar{\theta}_i}^0 \frac{dh}{\min(-(c_0+c_1h+c_2h^2),0)-\tau_i}$, which is equivalent to (17). ■

Remark 4: We can calculate $t^i_{\min}$ through either numerical integration, or analytical integration. If $c_0 + c_1 h + c_2 h^2 \geq 0,\ h \in [0, \bar{\theta}_i]$, the analytical integration depends on the the discriminant of $(c_0+\tau_i)+c_1h+c_2h^2 = 0$. Denote its roots as h_1 and h_2. Notice that if $c_0 + c_1h + c_2h^2 \geq 0$ then c_0, c_1, c_2 are all positive and $(c_0+\tau_i)+c_1h+c_2h^2 > 0$, and thus $t^i_{\min}$ can be written in (19).

$$t^i_{\min} = \begin{cases} \dfrac{1}{c_2(h_1 - h_2)}\ln\left(\dfrac{h_2(\bar{\theta}_i - h_1)}{h_1(\bar{\theta}_i - h_2)}\right) & \text{if } \Delta > 0 \\ -\dfrac{1}{c_2}\left(\dfrac{1}{h_1} + \dfrac{1}{\bar{\theta}_i - h_1}\right) & \text{if } \Delta = 0 \\ \dfrac{2}{\sqrt{-\Delta}}\left[\arctan\left(\dfrac{2c_2}{\sqrt{-\Delta}}\bar{\theta}_i + \dfrac{c_1}{\sqrt{-\Delta}}\right)\right. & \\ \left. -\arctan\left(\dfrac{c_1}{\sqrt{-\Delta}}\right)\right] & \text{if } \Delta < 0 \end{cases} \tag{19}$$

where $\Delta = c_1^2 - 4c_2(c_0 + \tau_i)$.

Corollary 2 implies that the Zeno behavior of the proposed DETM is excluded. By adjusting the value of $\bar{\theta}_i$, we can vary the MIET and keep the communication frequency consistently lower than $1/t^i_{\min}$. Increasing the value of $\bar{\theta}_i$ enables the inter-event time much longer to prevent overloading the communication network. The theoretical limit of the most prolonged $t^i_{\min}$ is determined by the limit of (19) when $\bar{\theta}_i$ tends to positive infinity. Indeed, a smaller $\bar{\theta}_i$ could also be designed to keep better surveillance and a higher data transmission rate if the network allows it. Therefore, by choosing an appropriate parameter $\bar{\theta}_i$, the control performance and the communication frequency could achieve a good compromise.

IV. SIMULATIONS

Consider a MAS with four follower agents and one leader. These agents could present wheeled mobile robots whose dynamics are defined in (1) with the following matrices:

$$\boldsymbol{A} = \begin{pmatrix} 0 & 0 & 1 & 0 \\ 0 & 0 & 0 & 1 \\ 0 & 0 & 0 & 0 \\ 0 & 0 & 0 & 0 \end{pmatrix}, \boldsymbol{B} = \begin{pmatrix} 0 & 0 \\ 0 & 0 \\ 1 & 0 \\ 0 & 1 \end{pmatrix}, \boldsymbol{C} = \begin{pmatrix} 1 & 0 \\ 0 & 1 \\ 0 & 0 \\ 0 & 0 \end{pmatrix}^T \tag{20}$$

These matrices are widely used for mobile robots such as in [12], [18]. Denote $\boldsymbol{x}_i = [p_{xi}, p_{yi}, v_{xi}, v_{yi}]^T$ where p_{xi}, p_{yi} are the position components along X and Y axes, and v_{xi}, v_{yi} are the linear velocity components along X and

Y axes. The agents' initial conditions are set as $\boldsymbol{x}_0(0) = [-1\ 1.5\ 0.5\ 1]^T$, $\boldsymbol{x}_1(0) = [-2\ 0\ 0\ 0]^T$, $\boldsymbol{x}_2(0) = [0\ 2\ 0\ 0]^T$, $\boldsymbol{x}_3(0) = [0\ 1\ 0.1\ 0]^T$, $\boldsymbol{x}_4(0) = [2\ 2\ 0\ 0]^T$. The initial states of observers are set as 0.

Consider a directed communication topology described in Fig.1. The corresponding augmented graph $\bar{\mathcal{G}}$ satisfies Assumption 3.

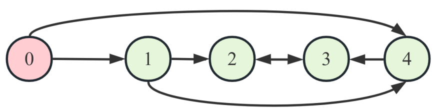

Fig. 1. Communication topology

Set $b_1 = b_2 = 1$ and we obtain the following solution of the gain of controllers $\boldsymbol{K}$ and the gain of observers $\boldsymbol{L}_o$:

$$\boldsymbol{K} = \begin{pmatrix} 0.0722 & 0 & 0.9545 & 0 \\ 0 & 0.0722 & 0 & 0.9545 \end{pmatrix} \tag{21}$$

$$\boldsymbol{L}_o = \begin{pmatrix} -1.40 & 0 & -9.49 & 0 \\ 0 & -1.00 & 0 & -1.25 \end{pmatrix}^T \tag{22}$$

Notation: in following figures, x_{ji} denotes the j-th component of agent i's vector $\boldsymbol{x}$.

Set $\bar{\theta}_i = 10, i = 1, ..., 4$. The trajectories of consensus error within 60 seconds are shown in Fig.2. It can be seen that the consensus is well achieved, and Fig.3 illustrates the control inputs of each agent.

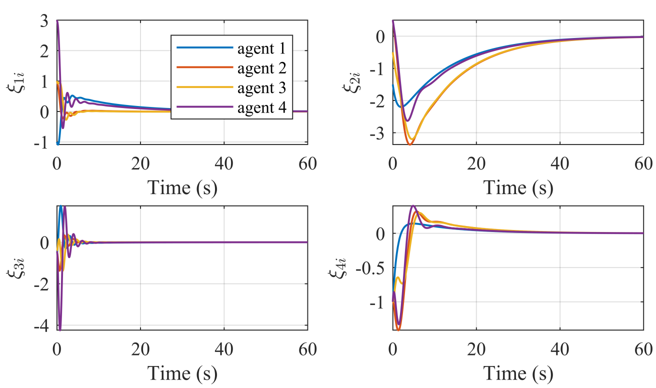

Fig. 2. Consensus error of follower agents. ξ_{ji} denotes the j-th component of agent i's consensus error vector $\boldsymbol{\xi}$.

The time evolution of $\theta_i(t)$ is presented in Fig.4. We can see that $\theta_i(t)$ for each agent is asynchronous, and events occur at the discontinuous points where $\theta_i(t)$ is reset to $\bar{\theta}_i$, which shows a clock-like behavior. Furthermore, Fig.5 plots event-triggered instants for each agent within 60 seconds. The density of the event occurrence varies with time, which during the initial stage (initial 5 seconds) is much denser than when the system is stable (approximately after 45 seconds).

Table.I presents the inter-event time with different $\bar{\theta}_i$ and also the inter-event time under the static event-triggered mechanism (SETM). For SETMs, the Lyapunov function is the same as in the proof of Theorem 1 by taking $\boldsymbol{\Theta} = \boldsymbol{I}_N, \dot{\boldsymbol{\Theta}} = \boldsymbol{0}$, which finally leads to a static event-triggered rule. The IET increases with larger $\bar{\theta}_i$ and can be easily tuned to be longer than the SETM. Therefore, by appropriately adjusting $\bar{\theta}_i$, the IET can be changed according to requirements, which demonstrates the significant advantage of the proposed method compared to the existing SETM.

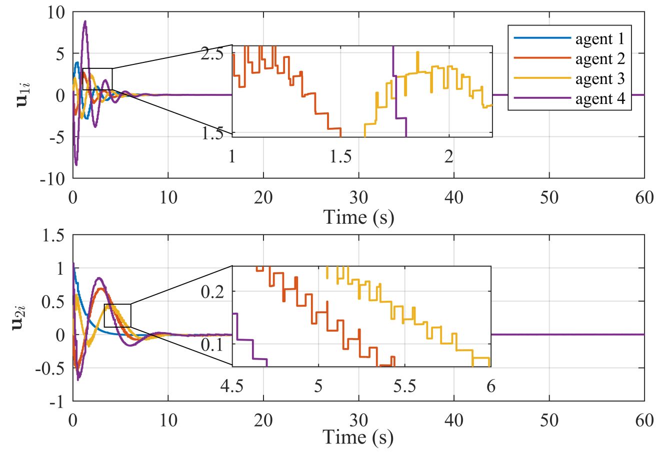

Fig. 3. Control input of follow agents. u_{ji} denotes the j-th component of agent i's control input vector $\boldsymbol{u}$.

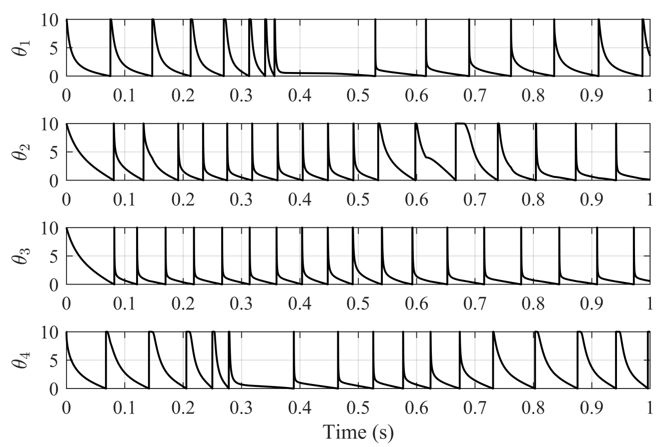

Fig. 4. Time evolution of auxiliary dynamic variables $\theta_i(t)$ of follower agents

Fig.6 plots $t^i_{\min}$ with different $\bar{\theta}_i$ using (17). The proposed DETM can prevent Zeno behavior as long as $\bar{\theta}_i > 0$. By adjusting $\bar{\theta}_i$, we can control the MIET and guarantee that the network communication is consistently below a designated frequency. Notice that $t^i_{\min}$ is only a lower bound of inter-event time and the actual inter-event time according to Table.I is much longer than the MIET, which only serves as an indicator in the worst case.

V. Conclusion

This paper presents a novel solution to the leader-following consensus problem in MASs under directed topology. The proposed solution aims to reduce the frequency of inter-agent information exchange by introducing a dynamic

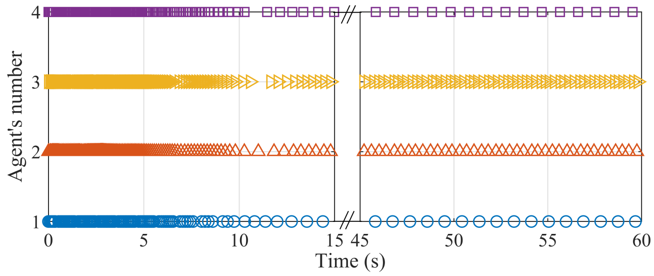

Fig. 5. Event-triggered instants of follower agents

TABLE I

INTER-EVENT TIME (IN MS) UNDER THE PROPOSED DETM STRATEGY AND THE SETM: MEAN VALUES (MEAN), MINIMUM VALUES (MIN) AND MAXIMUM VALUES (MAX) AMONG FOLLOWER AGENTS.

Case	$\bar{\theta}_i = 0.1$	$\bar{\theta}_i = 1$	$\bar{\theta}_i = 10$	$\bar{\theta}_i = 100$	SETM
Mean	41.8	216.6	284.4	295.2	37.2
Min	21.4	169.0	208.3	219.8	18.6
Max	86.6	291.3	400.0	402.7	69.4

event-triggered control protocol. This protocol allows for the design of the inter-event time, and an explicit expression for the minimum inter-event time is provided, which enables more flexible tuning and prevents Zeno behavior. Additionally, model-based estimation and clock-like auxiliary dynamic variables prolong the inter-event time as much as possible. The co-design of distributed controllers/observers using the $\mathcal{LMI}$ approach is a novel contribution that further distinguishes this study. The simulation results demonstrate a significant improvement in enlarge the communication interval compared to the static event-triggered methods, showcasing the effectiveness of the proposed solution. Future work will focus on extending these methods for consensus problems of MASs that are subject to faults and switching topology.

REFERENCES

[1] W. Ni and D. Cheng, "Leader-following consensus of multi-agent systems under fixed and switching topologies," *Systems & Control Letters*, vol. 59, no. 3–4, pp. 209–217, Mar 2010.

[2] C. Wang, L. Zhang, and F. Cao, "Leader-following consensus control of second-order nonlinear multi-agent systems with applications to slew rate control," *Asian Journal of Control*, pp. 1–9, 2022.

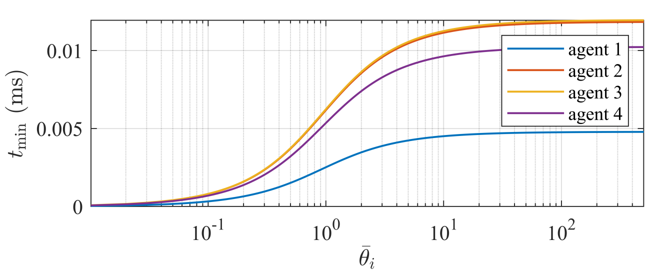

Fig. 6. Minimum inter-event time $t^i_{\min}$ with different $\bar{\theta}_i$ using (17).

[3] H. Guo, M. Meng, and G. Feng, "Mean square leader-following consensus of heterogeneous multi-agent systems with markovian switching topologies and communication delays," *International Journal of Robust and Nonlinear Control*, vol. 33, no. 1, pp. 355–371, 2023.

[4] S.-M. Kang and H.-S. Ahn, "Design and realization of distributed adaptive formation control law for multi-agent systems with moving leader," *IEEE Transactions on Industrial Electronics*, vol. 63, no. 2, pp. 1268–1279, 2016.

[5] A. Qiu, A. W. Al-Dabbagh, and T. Chen, "A tradeoff approach for optimal event-triggered fault detection," *IEEE Transactions on Industrial Electronics*, vol. 66, no. 3, pp. 2111–2121, 2019.

[6] P. Tabuada, "Event-triggered real-time scheduling of stabilizing control tasks," *IEEE Transactions on Automatic Control*, vol. 52, p. 1680–1685, 2007.

[7] W. Qi, C. Zhang, G. Zong, S.-F. Su, and M. Chadli, "Finite-time event-triggered stabilization for discrete-time fuzzy markov jump singularly perturbed systems," *IEEE Transactions on Cybernetics*, pp. 1–10, 2022.

[8] Y. Wu, X. Yang, H. Yan, M. Chadli, and Y. Wang, "Adaptive fuzzy event-triggered sliding mode control for uncertain euler-lagrange systems with performance specifications," *IEEE Transactions on Fuzzy Systems*, pp. 1–13, 2022.

[9] A. Girard, "Dynamic triggering mechanisms for event-triggered control," *IEEE Transactions on Automatic Control*, vol. 60, no. 7, p. 1992–1997, Jul 2015.

[10] X. Wu, B. Mao, X. Wu, and J. Lu, "Dynamic event-triggered leader-follower consensus control for multiagent systems," *SIAM Journal on Control and Optimization*, vol. 60, no. 1, p. 189–209, Feb 2022.

[11] Y. Yang, D. Yue, and C. Xu, "Dynamic event-triggered leader-following consensus control of a class of linear multi-agent systems," *Journal of the Franklin Institute*, vol. 355, no. 15, p. 7706–7734, Oct 2018.

[12] X. Ge and Q.-L. Han, "Distributed formation control of networked multi-agent systems using a dynamic event-triggered communication mechanism," *IEEE Transactions on Industrial Electronics*, vol. 64, no. 10, pp. 8118–8127, 2017.

[13] J. Berneburg and C. Nowzari, "Distributed dynamic event-triggered coordination with a designable minimum inter-event time," in *2019 American Control Conference (ACC)*, 2019, pp. 1424–1429.

[14] Z. Wang and M. Chadli, "Improved dynamic event-triggered consensus control for multi-agent systems with designable inter-event time*," in *2023 31st Mediterranean Conference on Control and Automation (MED)*, 2023, pp. 818–823.

[15] X. Chu, N. Huang, and Z. Sun, "Event triggering control for dynamical systems with designable inter-event times," *IFAC-PapersOnLine*, vol. 53, no. 2, p. 6410–6415, 2020.

[16] H. Zhang, G. Feng, H. Yan, and Q. Chen, "Observer-based output feedback event-triggered control for consensus of multi-agent systems," *IEEE Transactions on Industrial Electronics*, vol. 61, no. 9, pp. 4885–4894, 2014.

[17] J. Hu, J. Geng, and H. Zhu, "An observer-based consensus tracking control and application to event-triggered tracking," *Communications in Nonlinear Science and Numerical Simulation*, vol. 20, no. 2, pp. 559–570, 2015.

[18] G. Zhu, K. Liu, H. Gu, W. Luo, and J. Lü, "Observer-based event-triggered formation control of multi-agent systems with switching directed topologies," *IEEE Transactions on Circuits and Systems I: Regular Papers*, vol. 69, no. 3, pp. 1323–1332, 2022.

[19] J. A. V. Trejo, M. Chadli, D. Rotondo, M. A. Medina, and D. Theilliol, "Event-triggered fault-tolerant leader-following control for homogeneous multi-agent systems," *IFAC-PapersOnLine*, vol. 55, no. 6, p. 79–84, 2022.

[20] X. Ruan, J. Feng, C. Xu, and J. Wang, "Observer-based dynamic event-triggered strategies for leader-following consensus of multi-agent systems with disturbances," *IEEE Transactions on Network Science and Engineering*, vol. 7, no. 4, pp. 3148–3158, 2020.

[21] C. B. Yu, J. Qin, and H. Gao, "Cluster synchronization in directed networks of partial-state coupled linear systems under pinning control," *Automatica*, vol. 50, no. 9, pp. 2341–2349, 2014.

[22] E. Garcia, Y. Cao, and D. W. Casbeer, "Decentralized event-triggered consensus with general linear dynamics," *Automatica*, vol. 50, no. 10, p. 2633–2640, Oct 2014.